

**Ferroelectric distortions in doped ferroelectrics: BaTiO<sub>3</sub>:M (M = V–Fe)**Hirak Kumar Chandra,<sup>1</sup> Kapil Gupta,<sup>1</sup> Ashis Kumar Nandy,<sup>1,2</sup> and Priya Mahadevan<sup>1</sup><sup>1</sup>*Department of Condensed Matter Physics and Material Sciences, S.N. Bose National Centre for Basic Sciences, Block JD, Sector-III, Saltlake, Kolkata 700098, India*<sup>2</sup>*Indian Association for the Cultivation of Science, Jadavpur, Kolkata 700032, India*

(Received 29 April 2011; revised manuscript received 6 May 2013; published 27 June 2013)

A major challenge in the search for multiferroic materials among transition metal compounds has been that ferroelectricity is primarily found in  $d^0$  materials while magnetism is found in  $d^n$  systems. Considering a well-known ferroelectric oxide, namely BaTiO<sub>3</sub>, the question we asked within a theoretical study was whether ferroelectric distortions disappeared for the slightest amount of doping. Surprisingly, in the case of V-doped BaTiO<sub>3</sub>, ferroelectricity was found to be stronger than in the undoped limit. Another surprise was that the presence of charged impurities rather than free carriers was found to be most detrimental to the presence of ferroelectric distortions. These ideas of the low doping limit were used to design alternative multiferroics.

DOI: [10.1103/PhysRevB.87.214110](https://doi.org/10.1103/PhysRevB.87.214110)

PACS number(s): 77.80.–e, 71.20.–b, 71.55.Ht, 77.84.Cg

**I. INTRODUCTION**

The simultaneous presence of magnetism and ferroelectricity in the same material has become an active area of research over the past decade or so.<sup>1</sup> The prospect of being able to switch magnetism by an electric field and the electric polarization by a magnetic field has been actively investigated for possible device applications.<sup>2</sup> The problem, however, emerges from the fact that there are very few examples of materials<sup>3</sup> that simultaneously exhibit the two types of order, and even if they are found, the electric polarization is orders of magnitude smaller than conventional ferroelectrics (FEs) in most cases. Restricting ourselves to transition metal compounds, one finds that magnetism requires a finite  $d$  electron count. The largest FE polarizations are, however, observed in  $d^0$  compounds.<sup>4,5</sup> In those compounds where one has a finite  $d$  count, ferroelectricity emerges from spin spiral magnetic configurations,<sup>6</sup> geometric effects,<sup>7</sup> charge ordering,<sup>8</sup> etc. and usually has a small ionic displacement component. The typical values of polarizations are, however, orders of magnitude smaller.

An obvious route to high FE polarizations emerges from these observations. The off-centric distortions that one observes in  $d^0$  FEs are responsible for the large values of electric polarizations. So if one could look for examples of materials which have  $d^0$ -type distortions at a finite  $d$  electron number, this could serve as a route to multiferroics. The problem that one encounters is that the nature of the distortions that one finds in  $d^0$  systems is not found when one has a finite  $d$  electron count. This remains a general observation, although there is nothing which disallows both types of distortions to exist simultaneously. To examine this, we studied the stabilization of  $d^0$ -type distortions as electrons were doped into a well-known FE, namely BaTiO<sub>3</sub>. Our choice of dopant atoms was the  $3d$  transition metal ( $M$ ) atoms, as we could then have both magnetism and ferroelectricity. These systems have been investigated experimentally, but the existence of ferroelectricity is clouded by experimental uncertainties.<sup>9,10</sup>

The  $d^0$  distortions are associated with second-order Jahn-Teller effects. So, a route that seems to have recently emerged successfully for ferroelectricity in finite  $d$  electron systems is to quench first-order Jahn-Teller effects, so that only

second-order effects become operative.<sup>11</sup> Our analysis of doped BaTiO<sub>3</sub> revealed surprises. In spite of carrier doping, all examples of transition metal doping in which the doped electrons occupied a filled impurity band were found to favor a FE state. Even in cases in which the doped carriers occupied a partially filled impurity band, the off-centric distortions (OFDs) survived,<sup>12</sup> resulting in the uncommon example of a ferroelectric metal.<sup>13</sup> To probe this further, we examined the nature of the distortions for an electron or hole homogeneously distributed in the conduction or valence band of BaTiO<sub>3</sub>. To examine this aspect, we considered supercells of BaTiO<sub>3</sub> and looked at doping percentages of 5.5–11 %. In spite of better screening being expected, OFDs were found to survive. Our results for Fe doping suggested that charged ions were found to destabilize the OFD more than free carriers. The most surprising result was found for V doping. A microscopic analysis revealed that in a  $d^1$  system, one would require an off-centric displacement larger than what is found in a BaTiO<sub>3</sub> system to sustain ferroelectricity. As the Coulomb interaction between electrons on the  $M$  atom and the neighboring oxygen is going to increase substantially, the question becomes how would the enhanced off-centering be sustained. Part of the energy stability we show comes from first-order Jahn-Teller effects. The basic ideas of the low doping limit are used to design bulk multiferroics. For a single VO<sub>2</sub> layer sandwiched between BaTiO<sub>3</sub>, we find FE distortions strongly stabilized in addition to ferromagnetism. The calculated polarization comes out to be of the same order of magnitude as  $d^0$  FEs.

**II. METHODOLOGY**

Ninety-atom supercells of BaTiO<sub>3</sub> ( $3 \times 3 \times 2$  repetition of the primitive tetragonal cell) were considered in which one Ti atom was replaced by a single  $M$  atom. The dopant atom was varied from V to Fe, translating into a doping of  $\sim 5\%$ . By changing the  $M$  atom, one dopes a larger concentration of carriers into the system. So, ferroelectricity is not expected to survive. The energies of the supercells with OFDs were compared with those found in the paraelectric unit cell to discuss the stability of the ferroelectric state. To contrast the results with the case in which the carrier was homogeneously

TABLE I. FE stabilization energies for various doping in a  $3 \times 3 \times 2$  supercell of  $\text{BaTiO}_3$  within GGA +  $U$ . The experimental cell parameters are used for the primitive cell, while the internal positions have been optimized.

Doping element	FE stabilization energy (eV)
V	-0.523
Cr	0.038
Mn	-0.184
Fe	-0.152
No doping	-0.204
one electron	-0.085
two electrons	-0.001
one hole	-0.214
two holes	-0.194

distributed, calculations were performed with one to two extra carriers in the valence or conduction band of  $\text{BaTiO}_3$  (Table I). The lattice parameters of the unit cell were fixed at the experimental values of 3.997 and 4.031 Å (Ref. 14) for  $a$  and  $c$ , respectively. This is because of the fact that the generalized gradient approximation (GGA) optimized cells are known to overemphasize ferroelectricity. Using the experimental lattice parameters instead has been found to overcome such a deficiency. The experimental values for the atomic positions were taken for the ferroelectric as well as the paraelectric unit cells of  $\text{BaTiO}_3$ , and the internal coordinates were relaxed to get the minimum energy configuration. While rotations of the  $\text{TiO}_6$  octahedra are not encountered in  $\text{BaTiO}_3$ , they are often found in other transition-metal oxides, and we have allowed for that within our calculations. However, the rotations of the octahedra do not survive after optimizing the internal positions.

The electronic structure was solved within a plane-wave pseudopotential implementation of density functional theory as implemented in VASP<sup>15</sup> with projector augmented wave (PAW)<sup>16</sup> potentials. Spin-polarized calculations were performed for the doped cases. A  $k$ -point mesh of  $4 \times 4 \times 6$  was used for the calculations, and a cutoff energy for the plane waves was taken to be 400 eV. These values for the  $k$  points and the cutoff energy were found to be converged, as is evident from Table II. The case of single electron doping in the supercell of  $\text{BaTiO}_3$  is the only case in which the metallic nature of the ground state requires a large number of  $k$  points as well as cutoff energies. GGA(PW91) +  $U$  (Ref. 17) calculations were performed with a  $U$  on the dopant transition metal site equal to 3, 3, 4, and 5 eV for V, Cr, Mn, and Fe, respectively, consistent with earlier estimates.<sup>18</sup> These results are not specific to the choice of  $U$  and are found to be robust in a reasonable range of  $U$ , as shown in Table III. The present results were not specific to the tetragonal cell or volume used here. The FE stabilization energies of different  $M$  doping in a  $\text{BaTiO}_3$  supercell when the unit cell is cubic, as well as a slight increase and decrease in the volume of the experimental tetragonal unit cell (Table IV), have been calculated. It has been seen that ferroelectric distortion survives even when the unit cell is cubic as well as when the volume is changed within a reasonable range. Doping of  $M$  or carriers in  $\text{BaTiO}_3$  could

TABLE II.  $k$  points and cutoff energy convergence of FE stabilization energies for various  $M$ /carrier doping in a  $3 \times 3 \times 2$   $\text{BaTiO}_3$  supercell. The experimental cell parameters are used for the primitive cell, while the internal positions have been optimized.

Doping element	$k$ points	Energy cutoff (eV)	FE stabilization energy (eV)
V	$4 \times 4 \times 6$	400	-0.523
	$6 \times 6 \times 8$		-0.522
Cr	$4 \times 4 \times 6$	400	0.038
	$6 \times 6 \times 8$		0.039
Mn	$4 \times 4 \times 6$	400	-0.184
	$6 \times 6 \times 8$		-0.185
Fe	$4 \times 4 \times 6$	400	-0.152
	$6 \times 6 \times 8$		-0.152
one electron	$4 \times 4 \times 6$	400	-0.082
	$6 \times 6 \times 8$		-0.055
one hole	$4 \times 4 \times 6$	400	-0.210
	$6 \times 6 \times 8$		-0.207
V	$4 \times 4 \times 6$	400	-0.523
		600	-0.526
Cr	$4 \times 4 \times 6$	400	0.038
		600	0.038
Mn	$4 \times 4 \times 6$	400	-0.184
		600	-0.186
Fe	$4 \times 4 \times 6$	400	-0.152
		600	-0.156
one electron	$4 \times 4 \times 6$	400	-0.082
		600	-0.064
one hole	$4 \times 4 \times 6$	400	-0.210
		600	-0.214
one electron	$6 \times 6 \times 8$	400	-0.057
		600	

also modify the structure, so we have additionally optimized the volume in addition to the internal coordinates in those cases and examined the effect on the FE stability, and the results are reported in Table V. The volume changes and their effect on the observed ferroelectricity are small, so the discussion presented is for the case in which the primitive unit cell parameters are the same as the experimental cell unless otherwise specified.

Density functional calculations that use GGA and the local density approximation (LDA) for the exchange correlation

TABLE III. FE stabilization energy of  $M$ -doped  $3 \times 3 \times 2$   $\text{BaTiO}_3$  supercell for different  $U$  values. The experimental cell parameters are used for the primitive cell while the internal positions have been optimized.

Doping element	Value of $U$ (eV)	FE stabilization energy (eV)
V	2	-0.400
	3	-0.523
Cr	2	-0.028
	3	+0.038
Mn	4	-0.077
	3	-0.184
Fe	4	-0.184
	5	-0.151
	5	-0.152

TABLE IV. FE stabilization energy of  $M$  doping in a  $3 \times 3 \times 2$  supercell where the lattice parameters for the primitive unit cell are as specified. Internal positions have been optimized in each case.

Structure	Doping element	FE stabilization energy (eV)
Cubic unit cell	V	-0.447
( $a = 4.008 \text{ \AA}$ )	Cr	+0.106
at expt. volume	Mn	-0.097
Tetragonal unit cell	V	-0.623
( $a = 4.010, c = 4.045 \text{ \AA}$ ),	Cr	-0.273
1% increase from	Mn	-0.264
expt. volume	Fe	-0.223
Tetragonal unit cell	V	-0.439
( $a = 3.984, c = 4.018 \text{ \AA}$ ),	Mn	-0.110
1% decrease from	Fe	-0.091
expt. volume	V	-0.878
Tetragonal unit cell	Cr	-0.499
( $a = 4.037, c = 4.072 \text{ \AA}$ ),	Mn	-0.493
3% increase from	Fe	-0.422
expt. volume	V	-0.320
Tetragonal unit cell	Cr	-0.023
( $a = 3.957, c = 3.991 \text{ \AA}$ ),	Mn	-0.022
3% decrease from	Fe	-0.015
expt. volume		

functional have the drawback that they underestimate the band gap in most materials. Hybrid functional calculations have been seen to overcome this limitation. Therefore, the calculations were also performed using hybrid functionals, HSE06,<sup>19</sup> with a  $k$  mesh of  $2 \times 2 \times 4$ , and the results are shown in Table VI. Other details of the calculations are the same as the GGA +  $U$  calculations.

To understand the mechanism of ferroelectricity, we have used the interface of VASP to WANNIER90 (Ref. 20) to map the *ab initio* band structure onto a tight-binding model which includes  $d$  orbitals on the Ti and  $p$  orbitals on oxygen. The band energy has been calculated within this model for BaTiO<sub>3</sub> as well as electron-doped BaTiO<sub>3</sub>. The ideas of the dilute limit were used to search for new multiferroics based on these principles. For this purpose, we have considered a superlattice consisting of one layer of BaVO<sub>3</sub> sandwiched between 12 monolayers of BaTiO<sub>3</sub>. The experimental lattice parameters

TABLE V. The  $M$ -O bond lengths, change in volume, and FE stabilization energy after a complete optimization of the lattice parameters of an  $M$ -doped  $3 \times 3 \times 2$  BaTiO<sub>3</sub> supercell. All internal positions have been relaxed.

Doping element	$M$ -O bond lengths ( $\text{\AA}$ )	Change in volume (%)	FE stabilization energy (eV)
V	1.79, 2.10, 2.01 2.01, 2.01, 2.01	0.041	-0.526
Cr	1.85, 2.10, 1.99 1.99, 1.99, 1.99	0.219	0.030
Mn	1.90, 2.08, 1.97 1.97, 1.97, 1.97	0.327	-0.197
Fe	2.03, 2.08, 2.04 2.04, 2.04, 2.04	0.034	-0.154

TABLE VI. FE stabilization energies for various doping in a  $3 \times 3 \times 2$  BaTiO<sub>3</sub> supercell within HSE06. The experimental cell parameters are used for the primitive cell while the internal positions have been optimized.

Doping element	FE stabilization energy (eV)
V	-0.557
Cr	-0.445
Mn	-0.452
Fe	-0.310
No doping	-0.363

for BaTiO<sub>3</sub> were used here. We also allowed for rotation of the VO<sub>6</sub> octahedra and the structure was relaxed to reach the minimum energy configuration. No rotations were found in the relaxed structure. The electronic structure was solved using GGA +  $U$  potentials with other details the same as the bulk calculations. A  $k$ -point grid of  $6 \times 6 \times 1$  was considered for the calculations. Spheres of radii 1.0  $\text{\AA}$  were constructed around each atom in order to calculate the density of states (DOS). We use the Berry phase method<sup>21</sup> implemented in VASP to calculate the polarizations.

### III. RESULTS AND DISCUSSION

The stability of the FE state as a function of the doped  $M$  atom calculated within GGA +  $U$  is given in Table I. Surprisingly, FE or OFDs are found to survive in several instances, including V, Mn, and Fe with Born effective charges of 6.2 and 5.2 for V and Mn, significantly enhanced from the values expected for a 4+ valence state. In the case of Cr doping, however, one finds that the FE ground state is not favored. This immediately raises the question of what it is that differentiates between the different  $M$  dopings. The stabilization energy is large and equal to 523 meV for V, although it reduces to just 152 meV in the case of Fe doping. As a yardstick, we also give the FE stabilization energy in the absence of any doping in Table I, and we see that in the presence of V dopants, the energy is surprisingly enhanced by 319 meV. Such large stabilization energies would suggest that sizable FE distortions survive even in the doped case. This immediately raises the question of the nature of the distortions around the  $M$  site, as well as the mechanism by which the FE distortions survive and sometimes get enhanced in the present case. Before we examine the nature of the distortion in the presence of each  $M$  dopant that was considered, a brief review of the nature of distortion in undoped BaTiO<sub>3</sub> is useful. The Ti-O bond lengths in the absence of FE distortions are 2 and 2.015  $\text{\AA}$  in the  $xy$  plane and along the  $z$ , direction respectively. These get modified to 1.89 and 2.14  $\text{\AA}$  along the  $z$  direction as a result of Ti off-centering.

In Figs. 1(a) and 1(b), we examine the density of states for V-doped BaTiO<sub>3</sub>. The total density of states is plotted in panel (a) while the V  $d$  projected partial DOS is plotted in panel (b). The valence-band maximum (VBM) as well as the conduction-band minimum (CBM) have been indicated. These have been determined from O atoms (for the VBM) and Ti atoms (for the CBM) far away from the dopant atom as they

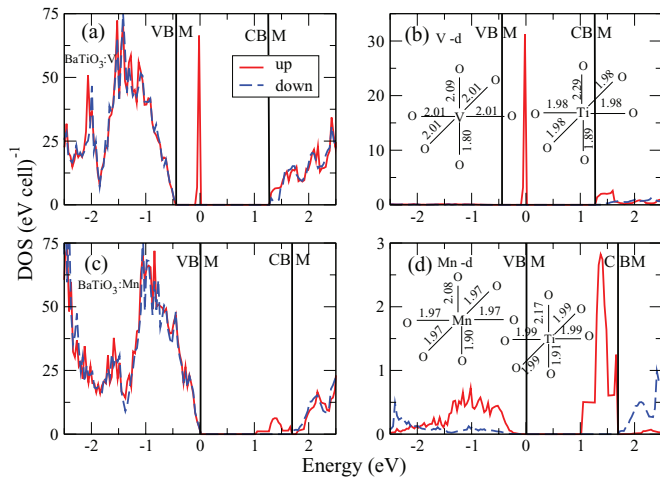


FIG. 1. (Color online) The up (solid line) and down (dashed line) spin total density of states for (a) V-doped BaTiO<sub>3</sub> and (c) Mn-doped BaTiO<sub>3</sub> calculated using GGA +  $U$  potentials is shown. The (b) V  $d$  and (d) Mn  $d$  projected partial density of states along with the position of the VBM and CBM have been indicated. The distortions of the VO<sub>6</sub> and MnO<sub>6</sub> octahedra as well as a Ti atom neighboring the V/Mn atom in the  $z$  direction are shown.

will be least perturbed by the  $M$  impurity. When a V atom substitutes for a Ti atom, it should have a  $d^1$  configuration. As is evident from panel (b), the single electron on V occupies a state in the band gap, while all other V associated states lie in the conduction band. The distortions of the VO<sub>6</sub> octahedron are shown in panel (b). One finds that while the bond lengths in the  $xy$  plane (henceforth called in-plane) are 2.01 Å, the bond lengths in the  $z$  direction (henceforth called out-of-plane) are 1.80 and 2.09 Å. For comparison, the distortions of the Ti-O bond lengths are given for a Ti atom (neighboring the V atom in the  $z$  direction). The expected first-order Jahn-Teller distortions for V in an octahedral geometry would involve two V-O bonds along the  $x$  axis becoming shorter while those along the  $y$  axis become longer or vice versa. The V-O bonds along the  $z$  axis remain at an intermediate value. Now in order to sustain this distortion in V-doped BaTiO<sub>3</sub>, the neighboring Ti atoms would be affected and therefore lose their off-centering and the relative energy cost is what drives V to have the FE distortions in the present case.

The large FE distortion that one finds for the VO<sub>6</sub> octahedron, larger than what is found in BaTiO<sub>3</sub>, is a surprise. To arrive at a microscopic understanding, we map the band structure of BaTiO<sub>3</sub> in the energy window 4 eV below the valence-band maximum and 3 eV above the conduction-band minimum to a tight-binding model which includes O  $p$  and Ti  $d$  as its basis states (Fig. 2). The band energy gain (difference in band energy of the FE and paraelectric structures) one finds from the *ab initio* calculation for this off-centric distortion is found to be 390 meV, of which the  $p$ - $d$  model accounts for 185 meV. Within the same  $p$ - $d$  model, keeping the distortions at the same value that one has for BaTiO<sub>3</sub>, we find that adding an extra electron to simulate a  $d^1$  system decreases the band energy gain to just 3 meV. So with the magnitude of Ti off-centering that one has in BaTiO<sub>3</sub>, one finds that a  $d^1$  system cannot sustain the FE distortion as the band

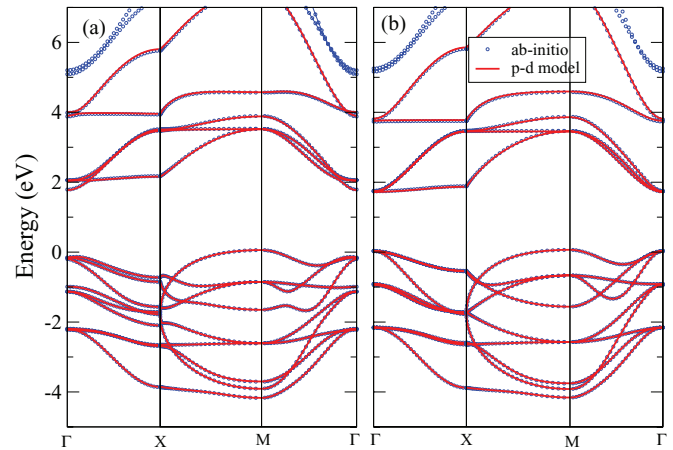


FIG. 2. (Color online) The *ab initio* (open blue circles) band dispersions calculated for BaTiO<sub>3</sub> using GGA potentials compared with the Wannier band structure (red solid lines) in a Ti  $d$ -O  $p$  model for (a) FE and (b) paraelectric structures. The zero of energy is compared to the valence-band maximum.

energy gain is very small. One would speculate that a shorter  $M$  (transition-metal)-O bond would be required as the band energy gain would be larger in that case. Indeed this is what our *ab initio* calculations find for V doped into a supercell of BaTiO<sub>3</sub>. The VO<sub>6</sub> octahedron gets distorted with one V-O bond length equal to 1.80 Å, less than what we have for BaTiO<sub>3</sub>. Using the local structure of the VO<sub>6</sub> octahedron within a bulk unit cell for BaTiO<sub>3</sub>, one finds that the band energy gain is now enhanced to 549 meV, higher than what one had for BaTiO<sub>3</sub>.

Now the question that follows is, why is such a short V-O distance sustained, as the increased Coulomb repulsion between the electrons should make it unfavorable. This emerges from a rather simple consequence. When V substitutes for Ti, it has a  $d^1$  electronic configuration, which would result in the Fermi level lying in the threefold-degenerate  $t_{2g}$  levels. One finds that the neighboring TiO<sub>6</sub> octahedra distort to allow the effective  $c/a$  for the VO<sub>6</sub> octahedron to be 0.97. This leads to a lifting of degeneracy of the  $t_{2g}$  orbitals with  $d_{xy}$  at lower energy and  $d_{yz}$  and  $d_{xz}$  at higher energy. The presence of a large exchange splitting at the V site ensures that the system is an insulator, which allows FE distortions to survive. So this enhanced tetragonality of the VO<sub>6</sub> octahedron found at this limit adds a first-order Jahn-Teller component to the energy, lowering it and thereby stabilizing the FE distortions. V doping does not introduce any free carriers with the single electron due to V occupying an impurity band in the band gap of BaTiO<sub>3</sub>. In spite of the increased stability of the ferroelectric state, the polarization that one finds is 15.3  $\mu\text{C}/\text{cm}^2$ . Although this is smaller than that found in BaTiO<sub>3</sub> (30  $\mu\text{C}/\text{cm}^2$ ),<sup>22</sup> this is significantly larger than most multiferroics.

Using these ideas of how ferroelectricity can be realized at the low doping limit, one examines if a similar  $c/a$  can be sustained in bulk tetragonal BaVO<sub>3</sub>. This is, however, not found to be the case and one finds no energy minimum in the case of bulk BaVO<sub>3</sub> in a structure that has FE distortions. However, a single layer of BaVO<sub>3</sub> sandwiched between 12 monolayers of BaTiO<sub>3</sub> is found to favor FE distortions with a calculated polarization as large as 16  $\mu\text{C}/\text{cm}^2$ . The

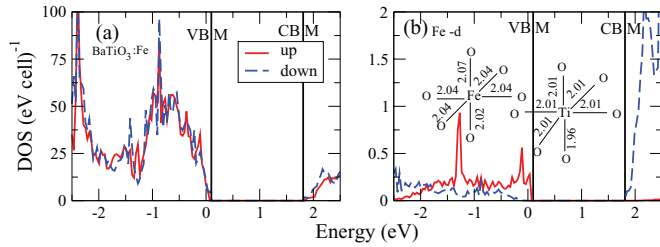


FIG. 3. (Color online) The up (solid line) and down (dashed line) spin (a) total density of states and (b) Fe  $d$  projected density of states for Fe-doped BaTiO<sub>3</sub> calculated using GGA +  $U$  are shown. The VBM and CBM have been indicated in addition to the distortions of the FeO<sub>6</sub> octahedron as well as those of the Ti atom neighboring the Fe atom in the  $z$  direction.

experimental lattice constants of BaTiO<sub>3</sub> were used for the superlattices. As the value of the  $c$  lattice parameter could be different for the VO<sub>2</sub> sandwich layer, we have started with the values corresponding to that for BaTiO<sub>3</sub> as well as a  $c/a$  of 0.97 which the dilute doping limit suggested. For the case in which the  $c/a$  ratio was equal to the value found in BaTiO<sub>3</sub>, the out-of-plane V-O bond lengths were found to be 1.91 and 2.14 Å, while for the case in which the  $c/a$  ratio was 0.97, the bond lengths were 1.92 and 2.11 Å. Allowing for magnetism, one finds that ferromagnetism is favored by 10 meV per V atom over the antiferromagnetic ground state. So this route of understanding ferroelectric distortions at the dilute limit has allowed us to design multiferroics which do not exist in the bulk limit but live en route.

Examining the case of Mn-doped BaTiO<sub>3</sub>, the system is again found to be insulating [Fig. 1(c)]. This is because Mn substituting for a Ti site is expected to have a configuration of  $d^3$ . The FE solution is lower in energy here also, although the stabilization energy is dramatically reduced. This is reflected by a smaller enhancement in the Born effective charge, which is found to be 5.2 from the expected value for the 4+ valence state. The polarization found here is found to be 22.6  $\mu\text{C}/\text{cm}^2$  with GGA +  $U$  potentials and 8.04  $\mu\text{C}/\text{cm}^2$  using Heyd-Scuseria-Ernzerhof (HSE) functionals.

All transition metal dopings that we have considered except Cr lead to a FE ground state. Considering the case of Cr doping in BaTiO<sub>3</sub>, we find that the structure which has no FE distortions is lower in energy (Table I).

The case of Fe doping in BaTiO<sub>3</sub> was found to be even more surprising. The OFD state was the ground state with an energy of stabilization of 152 meV. Fe is expected to have a formal  $d$  configuration of  $d^4$  if it isovalently substitutes the Ti site. However, what happens is that the majority spin Fe levels with  $t_{2g}$  and  $e_g$  symmetry are inside the valence band of BaTiO<sub>3</sub> (Fig. 3). This leads to the generation of a valence-band hole in addition to a configuration of  $d^5$  at the Fe site, i.e., a valence of Fe<sup>3+</sup>. A possible explanation for this is that the ionic radius for Fe<sup>4+</sup> is significantly smaller than that for Ti<sup>4+</sup> and so it favors the Fe<sup>3+</sup> valency when it substitutes Ti in BaTiO<sub>3</sub>. This

valence transition is analogous to what one found in Mn-doped GaSb.<sup>23</sup> The OFD stabilization energy is reduced by 62 meV from the value one obtained for a valence-band hole. This suggests that the presence of charged ions destabilizes OFDs more than free carriers.

Doping in BaTiO<sub>3</sub> could result in a change in the unit cell volume, although the changes are not expected to be very large at just 5% doping, as is evident from experimental reports.<sup>24</sup> The lattice parameters are optimized using *ab initio* calculations. The bond lengths, the change in volume from the experimental volume, and the FE stabilization energy of the optimized supercell have been given in Table V. It can be seen that the FE distortion as well as the FE stabilization energy of the optimized supercell are almost the same as that of the experimental supercell.

GGA calculations have the well-known drawback of underestimating the band gap in semiconductors and insulators, and this has been improved by the use of hybrid functionals.<sup>25</sup> This would in turn imply that the location of the impurity states associated with the  $M$  would be wrongly located in the band gap. To examine the effect of this on the FE stability, we calculated the electronic structure using hybrid functionals. The results are given in Table VI. Ferroelectricity was found to be favored for all the dopings considered. Cr doping, which was non-FE in the previous case, was now found to be FE. This was because the partially occupied impurity level which was doubly degenerate was split into two, with the unoccupied level being pushed to higher energies, thereby opening up a gap. As a result, Cr doping in the HSE calculations is similar to the V, Mn doping cases in which we have no free carriers. Fe doping transforms to a case in which the hole resides in an impurity band which is split off from the highest occupied level, and so a FE ground state is favored.

#### IV. CONCLUSION

These results illustrate several scenarios in which ferroelectricity will be favored upon doping BaTiO<sub>3</sub>. As long as the carriers are not free, we find that a FE ground state will be favored. Even when the carriers are free, OFD are favored for the counterintuitive case of more delocalized carriers. The presence of charged ions is found to destroy the OFD distortions more rapidly than free carriers. While naively one would expect the FE stabilization energy to decrease with doping, one finds that V doping leads to a state which has a higher FE stabilization energy than the undoped case, although the polarization is reduced. The dilute doping results are used to design bulk multiferroics.

#### ACKNOWLEDGMENTS

H.K.C. and P.M. thank the Department of Science and Technology, India. Part of the work is supported by the European Union FP7 program and the Department of Science and Technology under the Indo-EU project ATHENA.

<sup>1</sup>D. I. Khomskii, *J. Magn. Magn. Mater.* **306**, 1 (2006).

<sup>2</sup>R. Ramesh and N. A. Spaldin, *Nat. Mater.* **6**, 21 (2007).

<sup>3</sup>N. A. Hill, *J. Phys. Chem. B* **104**, 6694 (2000).

<sup>4</sup>R. E. Cohen, *Nature (London)* **358**, 136 (1992).

<sup>5</sup>L. Liang, Y. L. Li, L. Q. Chen, S. Y. Hu, and G. H. Lu, *J. Appl. Phys.* **106**, 104118 (2009).

- <sup>6</sup>Y. Yamasaki, S. Miyasaka, Y. Kaneko, J.-P. He, T. Arima, and Y. Tokura, *Phys. Rev. Lett.* **96**, 207204 (2006).
- <sup>7</sup>B. B. Van Aken, T. T. M. Palstra, A. Filippetti, and N. A. Spaldin, *Nat. Mater.* **3**, 164 (2004).
- <sup>8</sup>J. van den Brink and D. I. Khomskii, *J. Phys.: Condens. Matter* **20**, 434217 (2008).
- <sup>9</sup>S. Ray, P. Mahadevan, S. Mandal, S. R. Krishnakumar, C. S. Kuroda, T. Sasaki, T. Taniyama, and M. Itoh, *Phys. Rev. B* **77**, 104416 (2008).
- <sup>10</sup>R. Maier, J. L. Cohn, J. J. Neumeier, and L. A. Bendersky, *Appl. Phys. Lett.* **78**, 2536 (2001).
- <sup>11</sup>S. Bhattacharjee, E. Bousquet, and P. Ghosez, *Phys. Rev. Lett.* **102**, 117602 (2009); E. Bousquet, N. A. Spaldin, and P. Ghosez, *ibid.* **104**, 037601 (2010); J. H. Lee and K. M. Rabe, *ibid.* **107**, 067601 (2011).
- <sup>12</sup>In the case when the system is a metal, we refer to the distortions that survive as off-centric. While there may be a local polarization which is switchable, the macroscopic polarization vanishes.
- <sup>13</sup>P. W. Anderson and E. I. Blount, *Phys. Rev. Lett.* **14**, 7 (1965); T. Kolodiazny, M. Tachibana, H. Kawaji, J. Hwang, and E. Takayama-Muromachi, *ibid.* **104**, 147602 (2010).
- <sup>14</sup>G. H. Kwei, A. C. Lawson, S. J. L. Billinge, and S. W. Cheong, *J. Phys. Chem.* **97**, 2368 (1993).
- <sup>15</sup>G. Kresse and J. Furthmüller, *Phys. Rev. B* **54**, 11169 (1996).
- <sup>16</sup>G. Kresse and D. Joubert, *Phys. Rev. B* **59**, 1758 (1999).
- <sup>17</sup>S. L. Dudarev, G. A. Botton, S. Y. Savrasov, C. J. Humphreys, and A. P. Sutton, *Phys. Rev. B* **57**, 1505 (1998).
- <sup>18</sup>A. Chainani, M. Mathew, and D. D. Sarma, *Phys. Rev. B* **47**, 15397 (1993); T. Miyake and F. Aryasetiawan, *ibid.* **77**, 085122 (2008).
- <sup>19</sup>J. Heyd, G. E. Scuseria, and M. Ernzerhof, *J. Chem. Phys.* **118**, 8207 (2003); J. Heyd and G. E. Scuseria, *ibid.* **121**, 1187 (2004).
- <sup>20</sup>C. Franchini, R. Kováčik, M. Marsman, S. Sathyanarayana Murthy, J. He, C. Ederer, and G. Kresse, *J. Phys.: Condens. Matter* **24**, 235602 (2012).
- <sup>21</sup>R. W. Nunes and X. Gonze, *Phys. Rev. B* **63**, 155107 (2001).
- <sup>22</sup>W. Zhong, R. D. King-Smith, and D. Vanderbilt, *Phys. Rev. Lett.* **72**, 3618 (1994).
- <sup>23</sup>P. Mahadevan and A. Zunger, *Appl. Phys. Lett.* **85**, 2860 (2004).
- <sup>24</sup>J. R. Sambrano, E. Orhan, M. F. C. Gurgel, A. B. Campos, M. S. Goes, C. O. Paiva-Santos, J. A. Varela, and E. Longo, *Chem. Phys. Lett.* **402**, 491 (2005); T.-L. Phan, P. Zhang, D. Grinting, S. C. Yu, N. X. Nghia, N. V. Dang, and V. D. Lam, *J. Appl. Phys.* **112**, 013909 (2012).
- <sup>25</sup>R. Wahl, D. Vogtenhuber, and G. Kresse, *Phys. Rev. B* **78**, 104116 (2008).